Report

Current Biology

The CENP-A N-Tail Confers Epigenetic Stability to Centromeres via the CENP-T Branch of the CCAN in Fission Yeast

Highlights

- Cnp1/CENP-A N-tail mutants are viable but exhibit elevated chromosome loss
- N-tail mutants do not perturb Cnp1 loading or outer kinetochore assembly
- N-tail mutants exhibit centromere inactivation enhanced by an altered centromere
- N-tail mutants reduce the centromere levels of the CENP-T branch of the CCAN

Authors

H. Diego Folco, Christopher S. Campbell, ..., Shiv I.S. Grewal, Arshad Desai

Correspondence

abdesai@ucsd.edu

In Brief

Folco et al. show that the N-terminal tail of the centromeric histone variant Cnp1/CENP-A in fission yeast protects against centromere inactivation and chromosome loss. They link this epigenetic protection function to a role for the N-tail in targeting the CENP-T branch of the constitutive centromere-associated network to centromeres.

Accession Numbers

GSE63350

Folco et al., 2015, Current Biology *25*, 348–356
February 2, 2015
http://dx.doi.org/10.1016/j.cub.2014.11.060

CellPress

Current Biology 25, 348–356, February 2, 2015 ©2015 Elsevier Ltd All rights reserved http://dx.doi.org/10.1016/j.cub.2014.11.060

Report

The CENP-A N-Tail Confers Epigenetic Stability to Centromeres via the CENP-T Branch of the CCAN in Fission Yeast

H. Diego Folco,[1,3] Christopher S. Campbell,[1] Karen M. May,[2] Celso A. Espinoza,[1] Karen Oegema,[1] Kevin G. Hardwick,[2] Shiv I.S. Grewal,[3] and Arshad Desai[1,*]

[1]Ludwig Institute for Cancer Research, Department of Cellular and Molecular Medicine, University of California, San Diego, La Jolla, CA 92093, USA

[2]Wellcome Trust Centre for Cell Biology, Institute of Cell Biology, School of Biological Sciences, University of Edinburgh, Edinburgh EH9 3BF, UK

[3]Laboratory of Biochemistry and Molecular Biology, National Cancer Institute, NIH, Bethesda, MD 20892, USA

Summary

In most eukaryotes, centromeres are defined epigenetically by presence of the histone H3 variant CENP-A [1–3]. CENP-A-containing chromatin recruits the constitutive centromere-associated network (CCAN) of proteins, which in turn directs assembly of the outer kinetochore to form microtubule attachments and ensure chromosome segregation fidelity [4–6]. Whereas the mechanisms that load CENP-A at centromeres are being elucidated, the functions of its divergent N-terminal tail remain enigmatic [7–12]. Here, we employ the well-studied fission yeast centromere [13–16] to investigate the function of the CENP-A (Cnp1) N-tail. We show that alteration of the N-tail does not affect Cnp1 loading at centromeres, outer kinetochore formation, or spindle checkpoint signaling but nevertheless elevates chromosome loss. N-tail mutants exhibited synthetic lethality with an altered centromeric DNA sequence, with rare survivors harboring chromosomal fusions in which the altered centromere was epigenetically inactivated. Elevated centromere inactivation was also observed for N-tail mutants with unaltered centromeric DNA sequences. N-tail mutants specifically reduced localization of the CCAN proteins Cnp20/CENP-T and Mis6/CENP-I, but not Cnp3/CENP-C. Overexpression of Cnp20/CENP-T suppressed defects in an N-tail mutant, suggesting a link between reduced CENP-T recruitment and the observed centromere inactivation phenotype. Thus, the Cnp1 N-tail promotes epigenetic stability of centromeres in fission yeast, at least in part via recruitment of the CENP-T branch of the CCAN.

Results and Discussion

Cnp1 N-Tail Variants Support Viability but Exhibit Elevated Chromosome Missegregation

To investigate the function of the 20-amino-acid Cnp1 N-tail, we generated Halftail, Quartertail, and Deltatail variants and a Tailswap variant in which the Cnp1 N-tail was replaced by the N-tail of histone H3 (Figure 1A). All tested transgenes (either untagged or with GFP-coding sequence inserted immediately after the start codon) were inserted in single copy at the *lys1* locus (Figure 1A). We first assessed the ability of these variants to rescue lethality of *cnp1Δ* cells observed following 5-fluoroorotic acid (FOA)-mediated removal of plasmid-encoded *cnp1+* (Figure 1B). The *cnp1+*, *halftail*, *quartertail*, and *tailswap* transgenes rescued inviability, whereas *deltatail* did not (Figure 1B). Immunoblotting indicated that Deltatail was not expressed well (Figure S1A); consistent with this, overexpression of Deltatail rescued inviability of *cnp1Δ* and *cnp1^{ts}* (Figures S1B and S1C). Thus, the N-tail of Cnp1 is dispensable for viability of a *cnp1Δ* cell population.

We next assessed chromosome segregation fidelity using drug sensitivity and minichromosome loss assays. N-tail variants exhibited increased sensitivity to the microtubule-destabilizing drug thiabendazole (TBZ) (Figure 1C), with growth retardation approaching that observed for *clr4Δ*, a mutant of the H3K9 methyltransferase in which pericentromeric heterochromatin formation and cohesin enrichment are disrupted [17, 18]. TBZ sensitivity was not rescued by overexpression of Cnp1 N-tail variants (Figure S1D). Consistent with the increased TBZ sensitivity, Cnp1 N-tail variants exhibited high rates of loss of a nonessential 27 kb minichromosome (Figure 1D; the minichromosome carries an opal suppressor tRNA that complements a chromosomal *ade6-704* mutation; loss of the minichromosome results in red or sectored colonies) [19]; this phenotype was not observed when endogenous Cnp1 was present (Figure 1D).

To monitor endogenous chromosome segregation, we imaged septated cells (i.e., mostly S phase cells with two nuclei and calcofluor staining of the septum) harboring a GFP-marked LacO array insertion adjacent to the centromere of Chr II (referred to as *pericen2-lacO-gfp*). This analysis revealed elevated missegregation of endogenous Chr II in N-tail variants (Figure 1E). Thus, whereas N-tail variants of Cnp1 support viability of a cell population, they exhibit significantly elevated chromosome loss rates.

Cnp1 N-Tail Variants Are Normally Loaded at Centromeres and Support Outer Kinetochore Assembly

One explanation for the missegregation defect caused by alterations in the Cnp1 N-tail is a reduction in loading at centromeres. To test this possibility, we quantified the fluorescence at clustered centromeres of GFP-Cnp1, GFP-Halftail, and GFP-Tailswap in a *cnp1Δ* background. Both GFP-Halftail and GFP-Tailswap localized equivalently to GFP-Cnp1 at centromeres (Figures 1F and S1E). In addition, equivalent localization was observed for GFP-Cnp1 and N-tail variants, with the exception of Deltatail, in the presence of endogenous Cnp1 (Figure S1F). Consistent with their normal loading, overexpression of all Cnp1 N-tail variants rescued the temperature-sensitive growth defect of *scm3-139* (Figure S1G), which is caused by perturbation of the interaction between Cnp1 and its specialized chaperone Scm3 [20]. These results suggest that the elevated chromosome missegregation observed in the N-tail variants is not due to a defect in Cnp1 loading.

We next tested outer kinetochore assembly in the Cnp1 N-tail variants. First, we quantified centromere localization of the Ndc80 subunit of the conserved Ndc80 complex that directly mediates end-coupled microtubule attachments

*Correspondence: abdesai@ucsd.edu

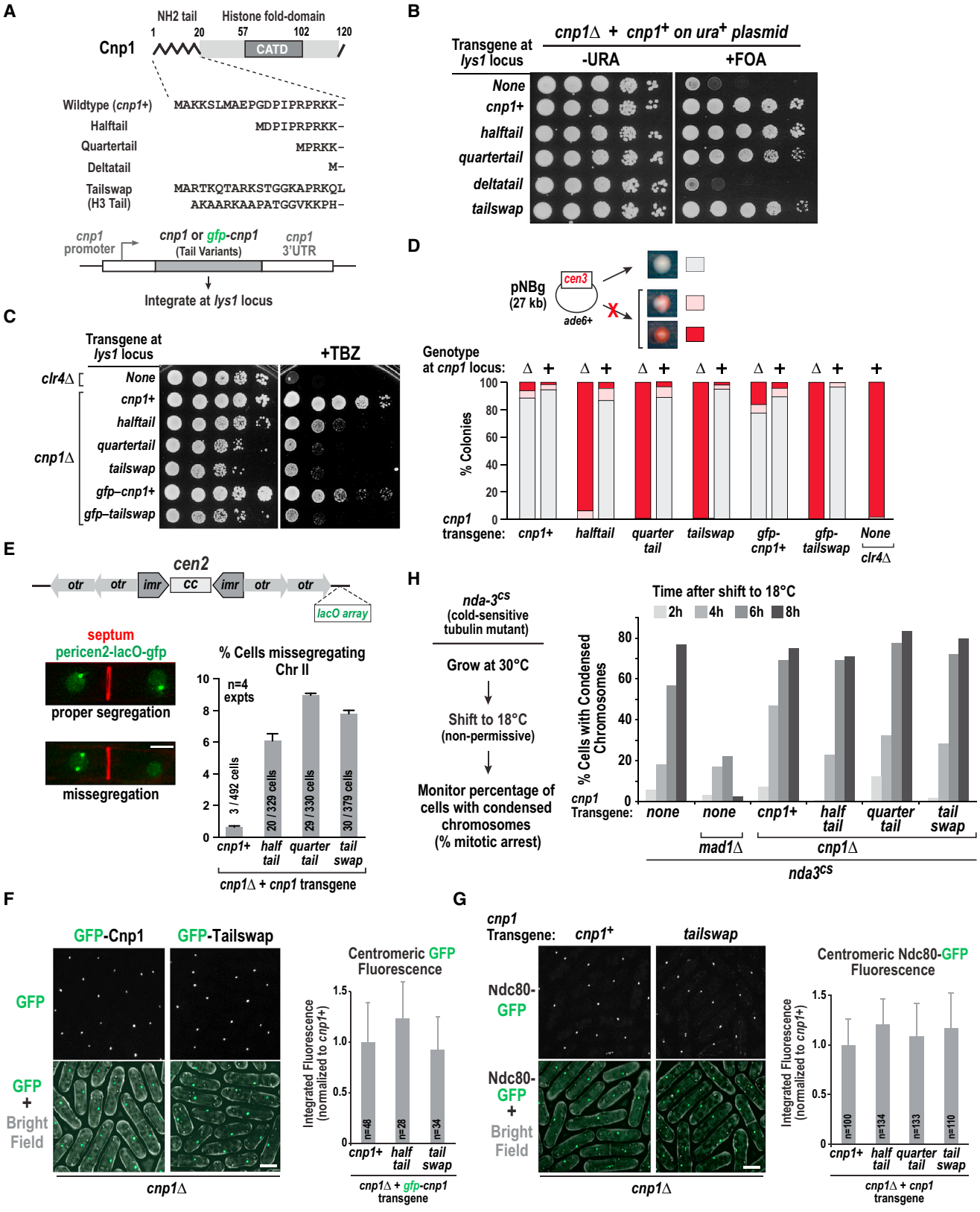

Figure 1. Cnp1 N-Tail Variants Support Viability, Centromere Loading, and Outer Kinetochore Formation yet Exhibit Elevated Chromosome Missegregation

(A) Schematic of the Cnp1 N-tail variants used in this study. All transgenes were integrated at the *lys1* locus.

(B) Plasmid shuffle assay, employing 5-fluoroorotic acid (5-FOA) to select against plasmid-encoded wild-type Cnp1, to analyze rescue of *cnp1*Δ cells by indicated transgenes. A 10-fold dilution series is shown for each condition.

(legend continued on next page)

[21, 22]. Ndc80 localization was unaffected in all tested N-tail Cnp1 variants (Figure 1G). Second, we monitored spindle checkpoint activity, which requires an intact outer kinetochore to generate a signal that prevents cell-cycle progression [23]. Analysis of the checkpoint-mediated arrest, performed using a cold-sensitive tubulin mutation to disrupt microtubules [24], revealed normal arrest in Cnp1 N-tail variants (Figure 1H); in contrast, the checkpoint pathway mutant *mad1Δ* failed to arrest. Thus, Cnp1 N-tail variants cause significant chromosome segregation defects, but these do not appear to arise from a problem in loading Cnp1 at centromeres or building an outer kinetochore with normal Ndc80 recruitment and checkpoint-signaling activity.

Cnp1 Tail Variants Exhibit Synthetic Lethality in the Presence of an Altered Central Core Sequence

A clue as to the origin of the Cnp1 N-tail variant missegregation defect came from a serendipitous observation made while introducing N-tail variants into strains harboring operator array insertions. Whereas we were able to construct strains expressing N-tail variants in a *cnp1Δ* background with operator array insertions outside the central core of the centromere (e.g., Figure 1E; Cnp1 is concentrated in the central core) [20, 25], we were unable to obtain strains with a TetO array insertion in the central core (Figure 2A; the strain also expresses a TetR-tomato fusion to label the array and is referred to as *cen2-tetO-tomato*) [26].

To assess if the N-tail variants and *cen2-tetO-tomato* were synthetic lethal, we used the mating-based random sporulation assay schematized in Figure 2A. In this assay, synthetic lethality is measured by the ratio of the number of colonies at 36°C (which prevents growth of *cnp1Δ* spores that inherited the *cnp1-1^{ts}* mutant transgene integrated at the *lys1* locus) versus 25°C (where *cnp1Δ* spores that inherit either the *cnp1-1^{ts}* mutant or a *gfp-cnp1* N-tail transgene integrated in the *lys1* locus form colonies). In the absence of a central core TetO array insertion and with a *gfp-cnp1+* transgene, the ratio was ~0.4, near the expected ratio of 0.5. The *cen2-tetO-tomato* insertion in combination with *gfp-cnp1+* reduced this ratio to ~0.2, indicating a mild synthetic defect. The *gfp-tailswap* transgene in the absence of a TetO insertion exhibited a ratio of 0.23. Strikingly, for the combination of *gfp-tailswap* and the TetO insertion, the ratio was <0.01, indicating strong synthetic lethality. Similar magnitude synthetic lethality was observed with *cen2-tetO-tomato* and *gfp-halftail* and *gfp-quartertail* transgenes (Figure 2A). Importantly, neither *cnp1-1^{ts}* (Figures 2B and S2A) nor *clr4Δ* (Figure 2C), which exhibits similar magnitude chromosome missegregation as the N-tail variants (Figure 1D), exhibited synthetic lethality with *cen2-tetO-tomato*. In addition, the observed synthetic lethality is not due to temperature sensitivity, as it was also observed in plasmid shuffle assays performed at 30°C (Figure 2C). Finally, synthetic lethality was not observed when N-tail variants were combined with an operator array integrated outside the central core (Figure S2B; Table S1). Thus, N-tail variants of Cnp1 exhibit strong synthetic lethality with a centromeric DNA sequence harboring an operator array insertion in the central core.

Rare Survivors Expressing Cnp1 N-Tail Variants and Harboring an Altered Central Core Sequence Exhibit Centromere Inactivation

Whereas the majority of cells expressing GFP N-tail variants in the presence of *cen2-tetO-tomato* were inviable, a small number of survivors were recovered (0.5%–1.0%; Figure 2A). To determine how these cells maintained viability, we imaged ten or more independent survivor colonies for two variants and found that the TetO-tomato focus was dissociated from the GFP focus and devoid of GFP signal (Figure 2D), suggesting loss of the N-tail variant Cnp1 from *cen2*. In agreement with the imaging data, anti-GFP chromatin immunoprecipitation (ChIP)-PCR (Figure S2C) and ChIP sequencing (ChIP-seq) analysis of a rare *gfp-tailswap*;*cen2-tetO-tomato* survivor colony showed complete loss of Cnp1 at the central core of *cen2* (Figure 2E). In addition, evidence for a neocentromere on Chr II was not observed in the ChIP-seq data, suggesting that these cells survive due to fusion of centromere-inactivated Chr II with one of the other two chromosomes, as previously observed following excision of a centromere [27]. To test this possibility, we performed pulsed-field gel electrophoresis, which indicated that Chr II had fused with Chr I in independent survivor colonies harboring different GFP-fused N-tail variants (Figures 2F and S2D).

Thus, combination of a Cnp1 N-tail variant with an array insertion at the central core results in centromere inactivation that, in the majority of cases, is lethal but in rare cases is tolerated through chromosome fusion. Similar synthetic lethality is not observed with *cnp1-1^{ts}* or *clr4Δ*, both of which compromise chromosome segregation. These observations suggest that Cnp1 N-tail variants increase the probability of centromere inactivation and that this effect is magnified by insertion of the TetO array in the central core.

Heterochromatin Occupies Inactivated Centromeres but Is Not Required for Centromere Inactivation

As the Cnp1-containing central core is flanked by pericentric heterochromatin, one possible mechanism for centromere inactivation is that heterochromatin encroaches into the

(C) Sensitivity of *cnp1Δ* cells expressing indicated Cnp1 N-tail variants to the spindle poison thiabendazole (TBZ). Growth was assayed at 30°C using 10-fold serial dilutions plated on rich yeast extract plus supplements (YES) medium with (right) or without (left) 10 μg/ml TBZ. *clr4Δ* serves as a TBZ-sensitive control.
(D) Minichromosome (pNBg) maintenance assay in wild-type and *cnp1Δ* (indicated as + or Δ, respectively) cells expressing Cnp1 N-tail variants. *clr4Δ* serves as a control with elevated missegregation. Cells with a minichromosome generate white colonies; minichromosome loss results in red or sectored colonies. Greater than 900 colonies were scored per condition.
(E) Segregation of Chr II marked with a pericentromeric LacO array labeled with LacI-GFP (*pericen2-lacO-gfp*). Septation was determined by calcofluor staining. Error bars are 95% confidence interval. The scale bar represents 3 μm.
(F) Images of *cnp1Δ* cells expressing GFP-tagged Cnp1 or Tailswap (left). The graph (right) plots the mean signal intensity of the GFP centromeric focus measured in large (lateG2) cells, normalized relative to wild-type GFP-Cnp1, for the indicated variants. Error bars are the SD. The scale bar represents 5 μm.
(G) Images of Ndc80-GFP in *cnp1Δ* cells expressing untagged Cnp1 or Tailswap. The graph (right) plots the mean signal intensity of the Ndc80-GFP centromeric focus measured in large (late G2) cells of the indicated variants, normalized relative to wild-type Cnp1. Error bars are the SD. The scale bar represents 5 μm.
(H) Left: assay used to monitor spindle checkpoint-dependent arrest. Cold-sensitive *nda3-KM311* (*nda3^{cs}*) strains, containing indicated deletions and integrations, were grown at 30°C and shifted to nonpermissive 18°C, and samples were fixed and processed for DAPI staining every 2 hr for 8 hr. Right: graph plotting the percentage of cells with condensed chromatin, a marker for mitotic arrest, at different times following shift to the nonpermissive temperature.

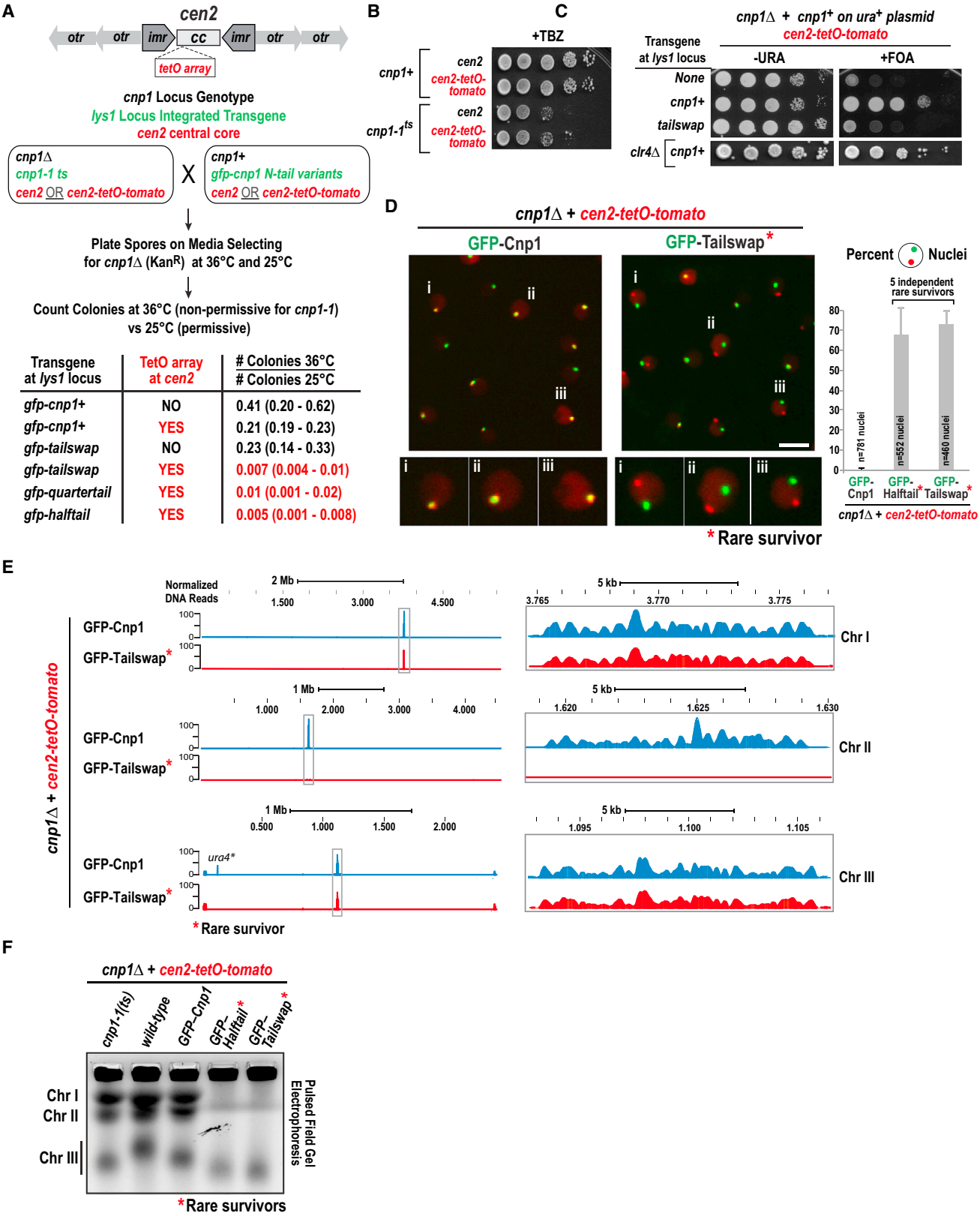

Figure 2. Cnp1 N-Tail Variants Are Unable to Propagate a Centromere Harboring a Repetitive TetO Array Insertion in the Central Core

(A) Schematic and results of mating and sporulation assay employed to assess synthetic lethality between GFP-tagged Cnp1 N-tail variants and the TetO array (*cen2-tetO-tomato*) insertion in the central core of centromere 2. Note that both partners in each mating harbored either unaltered *cen2* or *cen2-tetO-tomato*.

(legend continued on next page)

N-tail variant-containing central core. ChIP analysis revealed high levels of H3K9 methylation in the inactive centromere central core of the rare survivors (Figure 3A); in addition, a marker cassette inserted in this region was hypersilenced in the survivors (Figures S3A and S3B). To test if heterochromatin was required for centromere inactivation, we performed the mating-based assay in Figure 2A but with *clr4Δ* in both strains. No significant suppression of lethality was observed with *clr4Δ* (Figure 3B). Thus, heterochromatin is not required for centromere inactivation, but elevation of H3K9me2 in the central core provides an easy-to-measure readout for centromere inactivation events in a cell population.

Evidence for Centromere Inactivation in Cnp1 N-Tail Variant Cell Populations without Alterations in the Central Core Sequence

To test if centromere inactivation occurs with Cnp1 N-tail variants in the absence of any insertions in the central core, albeit with lower penetrance, we first performed ChIP followed by qPCR for presence of H3K9me2. This approach revealed a significant 2- to 4-fold increase in H3K9me2 in the central core in the presence of N-tail variants (Figures 3C and S3C). Based on the analysis in Figure 2, we suggest this elevation reflects inactivation of endogenous centromeres in a subset of the cell population that presumably leads to eventual lethality of the cells in which the inactivation event has occurred.

To assess centromere inactivation in single cells, we imaged septated GFP-Tailswap cells harboring a TetO array inserted adjacent to *cen1* (referred to as *pericen1-tetO-tomato*), which is not synthetically lethal with N-tail variants (Figure S2B; Table S1). We observed a significant frequency of two phenotypes: missegregation of *cen1* (12/262) and declustering of *cen1* from the other centromeres (33/262). Following missegregation, one of the two *cen1* foci was always declustered (12/12; Figure 3D). Notably, the missegregated and declustered centromeres exhibited highly reduced GFP signal, compared to the amount expected, indicating loss of Cnp1 from that centromere (Figure 3D). In a complementary approach, we imaged fields of cells over time. No missegregation of the *pericen1-tetO-tomato*-labeled chromosome was observed from imaging 175 GFP-Cnp1 divisions. From 457 GFP-Tailswap divisions, we could unambiguously score six events where both chromatids for Chr I segregated into one cell (Figure 3E; the low signal to noise of the *pericen1-tetO-tomato* marker makes this number an underestimate). In all six cases, one of the TetO-marked centromeres was declustered and did not exhibit GFP signal (Figure 3E, arrow), suggesting inactivation of the centromere on that chromatid.

Overall, both H3K9me2 ChIP-qPCR and imaging of single cells indicate that there is an elevated frequency of centromere-inactivation events in the presence of Cnp1 N-tail variants even in the absence of any alterations in central core sequence.

Cnp1 N-Tail Variants Selectively Reduce Centromeric Accumulation of the Cnp20/CENP-T Branch of the Inner Kinetochore

The increased probability of centromere inactivation in the absence of a loading defect led us to investigate the effect of Cnp1 N-tail variants on the chromatin-proximal region of the kinetochore. CENP-A nucleosomes primarily recruit Cnp3/CENP-C via their C-tail [28, 29] and, by an unknown mechanism, recruit the Cnp20/CENP-T branch of the constitutive centromere-associated network (CCAN) [30]. Cnp3/CENP-C localization at centromeres was only mildly affected by the tested N-tail variants (Figures 4A and 4B); in contrast, there was a striking and consistent reduction in Cnp20/CENP-T at centromeres (Figures 4A and 4B). We next monitored localization of Mis6/CENP-I and found that its reduction was comparable to Cnp20 reduction (Figures 4B and S4A). Thus, the CENP-T branch of the CCAN appears to be selectively diminished at centromeres in the Cnp1 N-tail variants, which likely underlies the increased probability of centromere inactivation and high rates of missegregation. As Ndc80 localization is unperturbed in the N-tail variants (Figures 1G and 1H), and *cnp20* mutants do not affect Ndc80 recruitment [31], this defect is potentially unrelated to the role of CENP-T family proteins in direct recruitment of the Ndc80 complex [32, 33].

We next test if overexpression of Cnp20/CENP-T suppressed phenotypic defects of N-tail variants. We overexpressed Cnp20/CENP-T in the Quartertail and Tailswap variants (in a *cnp1Δ* background) and monitored H3K9me2 accumulation at the central core and TBZ sensitivity to assess suppression. Cnp20 overexpression suppressed elevation of H3K9me2 in the central core in the presence of Quartertail (Figures 4C and S4B) and reduced TBZ sensitivity (Figure 4D). In contrast, we did not observe suppression of Tailswap by Cnp20 overexpression (Figures S4C and S4D). As Quartertail shares all of phenotypic features of the N-tail variants described here, these results suggest that the observed defects are primarily derived from reduced centromeric levels of the CENP-T branch of the CCAN. Tailswap may not be suppressed under the conditions tested either because it is more penetrant or because the presence of an H3 tail, a substrate for many modifications, has additional consequences.

Conclusions

The work described here implicates the N-tail of CENP-A in fission yeast in recruitment of the CENP-T branch of the CCAN and suggests that cooperation of Cnp1/CENP-A and

(B) TetO array insertion in the central core does not enhance TBZ sensitivity of *cnp1-1^{ts}*. Serial dilutions (10-fold) of indicated strains were plated on rich YES medium containing 10 μg/ml TBZ and grown at 30°C.

(C) Plasmid shuffle assay (10-fold serial dilutions) performed on the indicated strains. *clr4Δ* in combination with *cen2-tetO-tomato* and wild-type Cnp1 is shown below.

(D) Images of *cnp1Δ cen2-tetO-tomato* strains expressing GFP-Cnp1 (left) or GFP-Tailswap (right); the GFP-Tailswap and other N-tail variant strains analyzed were rare survivors isolated from the experiment in (A). The scale bar represents 5 μm; images on the bottom are magnified a further 2-fold. Graph on right plots percentage of cells displaying delocalization of green (GFP) and red (Tomato) foci. Five independent GFP-Halftail and GFP-Tailswap survivors were analyzed; error bars are the SD.

(E) GFP ChIP-seq of a control (GFP-Cnp1) and a GFP-Tailswap survivor in the *cnp1Δ cen2-tetO-tomato* background. All three *S. pombe* chromosomes are displayed. The y axis plots normalized read counts, with normalization relative to the number of mapped reads; the x axis is chromosomal position. The centromere regions (boxed) are enlarged on the right. Conventional duplex ChIP-PCR was also performed (see Figure S2C). The signal detected at the *ura4* locus (*ura4**) in GFP-Cnp1 is due to mapping of reads from the *ura4* marker inserted adjacent to *cen2-tetO-tomato*; as this centromere is inactivated in the GFP-Tailswap survivor, no *ura4* reads are mapped.

(F) Undigested chromosomal DNA samples from the indicated strains analyzed by pulsed-field gel electrophoresis. See also Figure S2D.

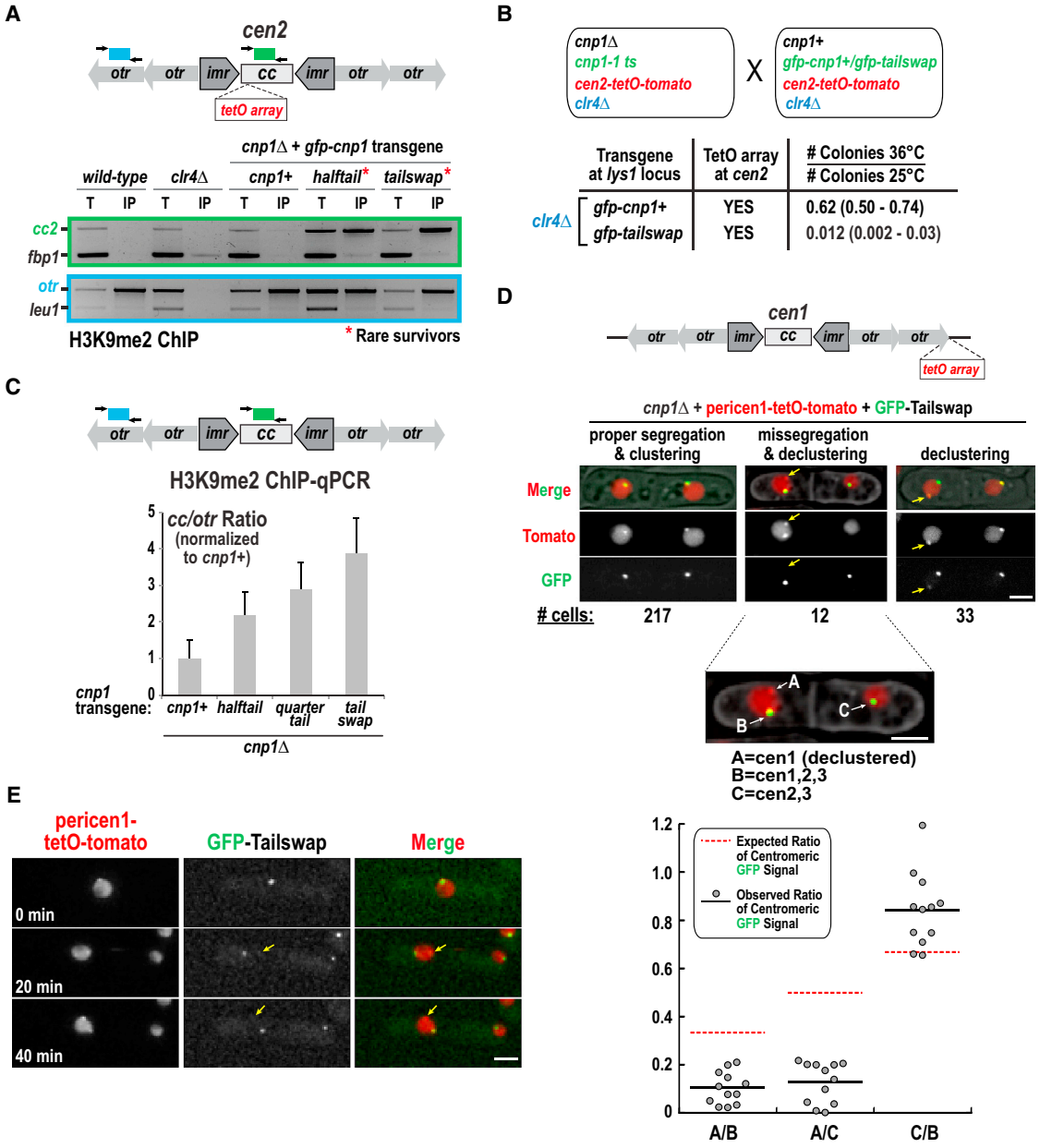

Figure 3. Evidence for Centromere Inactivation in Cnp1 N-Tail Variants in the Absence of Any Alterations in Centromeric DNA Sequence

(A) H3K9me2 ChIP-PCR analysis for the indicated strains. Centromere 2 (*cc2*) and heterochromatic outer repeats (*otr*) products were compared to noncentromeric controls *fbp1* and *leu1*, respectively. A *clr4*Δ control, which lacks H3K9me2, is also shown.

(B) Analysis of the effect of *clr4*Δ on synthetic lethality of GFP-Tailswap and *cen2-tetO-tomato*, conducted as in Figure 2A.

(C) H3K9me2 ChIP-qPCR for the indicated strains harboring unaltered centromeres. The normalized ratio between qPCR products from Cnp1 domains (central core 1 and 3 [*cc*]) and heterochromatic outer repeats (*otr*) is shown. Error bars represent the SD (n = 3). See also Figure S3C.

(D) Images of septated cells expressing GFP-Tailswap in a *cnp1*Δ background with a pericentromeric TetO array insertion (*pericen1-tetO-tomato*) on chromosome 1. The three classes of cells observed are indicated with the numbers for each class shown below the images. The yellow arrow marks the TetO-tomato focus that is declustered and has low GFP signal. In cells with missegregation and declustering, GFP intensity was measured at each red (TetO-Tomato) focus and the indicated ratios are plotted below. The expected ratio, assuming equal amount of GFP-Cnp1 is present at each centromere, is shown with a red dashed line. The scale bars represent 3 μm.

(E) Representative time-lapse images providing evidence for centromere inactivation. Arrow indicates a TetO-tomato focus that has very low GFP signal. The scale bar represents 3 μm.

Cnp20/CENP-T is important for stable centromere inheritance (Figure 4E). Whereas a prior study in human cells suggested that substitution of the CENP-A N-tail with the N-tail of H3 did not perturb CENP-T recruitment [11], this result may be due to a redundant contribution from the human centromeric alpha satellite sequence-specific DNA-binding protein CENP-B [11, 34–36].

As N-tail variants support viability, unlike a *cnp20* mutant [31], and do not eliminate Cnp20/CENP-T centromere localization, there must be additional Cnp20/CENP-T localization

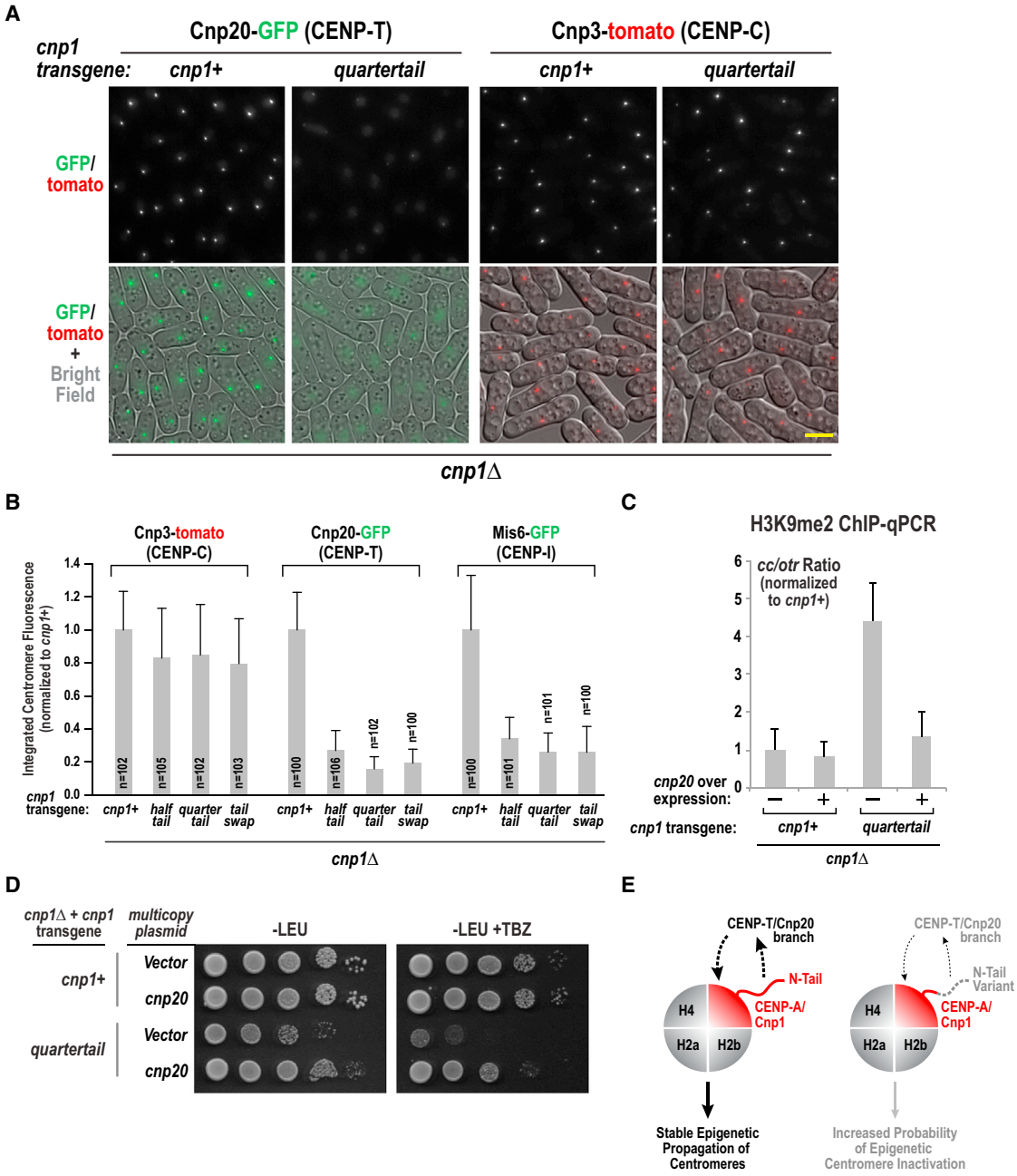

Figure 4. Cnp1 N-Tail Variants Selectively Reduce Centromeric Accumulation of the Cnp20/CENP-T Branch of the CCAN

(A) Representative images of Cnp20-GFP and Cnp3-tomato in the indicated strains. The scale bar represents 5 μm. See also Figure S4A.

(B) Integrated fluorescence intensity of Cnp20-GFP, Mis6-GFP, and Cnp3-tomato foci was measured and plotted for the indicate strains as in Figures 1F and 1G. Error bars represent the SD.

(C) ChIP-qPCR with H3K9me2 antibody for the indicated conditions. The normalized ratio of products from Cnp1-enriched regions (*cc*) and heterochromatic outer repeats (*otr*) is displayed. See also Figure S4B. Error bars represent the SD (n = 3).

(D) Serial dilutions of indicated strains harboring empty or Cnp20-overexpressing multicopy pREP1 plasmid were plated on minimal medium lacking leucine (PMG −LEU), with or without 15 μg/ml TBZ, and grown at 33°C. A 10-fold dilution series is shown for each strain.

(E) Schematic summary of key findings. The Cnp1/CENP-A N-tail is required to recruit the Cnp20/CENP-T branch of the CCAN, which in turn is required for stable epigenetic propagation of centromeres (left). Cnp1 N-tail variants are normally loaded and support outer kinetochore assembly, but the CENP-T branch of the CCAN is selectively reduced, increasing the probability of centromere inactivation and chromosome missegregation (right).

mechanisms. Recent work suggests that monomethylation of lysine 20 on histone H4 (H4K20me1) of CENP-A nucleosomes may be a mark for CENP-T recruitment in vertebrates [37]. However, deletion of the only known H4K20 methyltransferase in fission yeast does not cause increased TBZ sensitivity [38] and H4K20me1 is not enriched at the CENP-A-containing central core domain of the centromere (P. Svensson and K. Ekwall, personal communication). Future work is needed to assess if this modification of CENP-A nucleosomes plays a role in CENP-T recruitment outside of vertebrates. In addition, it will

be important to elucidate the biochemical nature of the Cnp1/CENP-A N-tail-Cnp20/CENP-T connection, as well as determine the precise timing and mechanisms responsible for the inactivation events observed in the N-tail variants with reduced Cnp20/CENP-T recruitment.

Experimental Procedures

Details of strain and plasmid construction, genetic analysis, imaging, and chromatin immunoprecipitations are provided in the Supplemental Experimental Procedures.

Accession Numbers

The NCBI GEO accession number for the Cnp1 ChIP-seq data reported here is GSE63350.

Supplemental Information

Supplemental Information includes Supplemental Experimental Procedures, four figures, and three tables and can be found with this article online at http://dx.doi.org/10.1016/j.cub.2014.11.060.

Author Contributions

H.D.F. designed and conducted the majority of the experiments with input from K.O. and A.D. K.M.M. and K.G.H. performed the spindle checkpoint analysis. C.S.C. performed the time-lapse imaging. C.A.E. performed the high-throughput sequencing and helped analyze the data. S.I.S.G. supported completion of the project. H.D.F. and A.D. wrote the manuscript with input from all authors.

Acknowledgments

We thank Shigeaki Saitoh and Kohta Takahashi (Kurume University); Alison Pidoux, Georgina Hamilton, and Robin Allshire (University of Edinburgh); Takeshi Sakuno and Yoshinori Watanabe (University of Tokyo); Oliver Limbo and Paul Russell (Scripps Institute); and the National BioResource Project - Yeast (Japan) for their generosity in sharing strains, plasmid, and expertise. We thank Bing Ren for supporting acquisition of the ChIP-seq data sets and Peter Svensson and Karl Ekwall (Karolinska Institute) and Ben Black and colleagues (University of Pennsylvania) for communicating unpublished results. This work was supported by NIH grant GM074215 to A.D. and the Intramural Research Program of the NIH to S.I.S.G. K.G.H. and K.M.M. were supported by a Wellcome Trust Programme Grant to K.G.H. (083610) and Wellcome Trust Centre for Cell Biology core grant 092076. C.A.E. was supported by NIH/NCI training grant T32 CA009523-27S1. A.D. and K.O. receive salary and other support from the Ludwig Institute for Cancer Research.

Received: October 3, 2014
Revised: November 17, 2014
Accepted: November 21, 2014
Published: January 22, 2015

References

1. Catania, S., and Allshire, R.C. (2014). Anarchic centromeres: deciphering order from apparent chaos. Curr. Opin. Cell Biol. *26*, 41–50.
2. Müller, S., and Almouzni, G. (2014). A network of players in H3 histone variant deposition and maintenance at centromeres. Biochim. Biophys. Acta *1839*, 241–250.
3. Fukagawa, T., and Earnshaw, W.C. (2014). The centromere: chromatin foundation for the kinetochore machinery. Dev. Cell *30*, 496–508.
4. Verdaasdonk, J.S., and Bloom, K. (2011). Centromeres: unique chromatin structures that drive chromosome segregation. Nat. Rev. Mol. Cell Biol. *12*, 320–332.
5. Perpelescu, M., and Fukagawa, T. (2011). The ABCs of CENPs. Chromosoma *120*, 425–446.
6. Cheeseman, I.M., and Desai, A. (2008). Molecular architecture of the kinetochore-microtubule interface. Nat. Rev. Mol. Cell Biol. *9*, 33–46.
7. Sullivan, K.F., Hechenberger, M., and Masri, K. (1994). Human CENP-A contains a histone H3 related histone fold domain that is required for targeting to the centromere. J. Cell Biol. *127*, 581–592.
8. Chen, Y., Baker, R.E., Keith, K.C., Harris, K., Stoler, S., and Fitzgerald-Hayes, M. (2000). The N terminus of the centromere H3-like protein Cse4p performs an essential function distinct from that of the histone fold domain. Mol. Cell. Biol. *20*, 7037–7048.
9. Takayama, Y., Sato, H., Saitoh, S., Ogiyama, Y., Masuda, F., and Takahashi, K. (2008). Biphasic incorporation of centromeric histone CENP-A in fission yeast. Mol. Biol. Cell *19*, 682–690.
10. Ravi, M., and Chan, S.W. (2010). Haploid plants produced by centromere-mediated genome elimination. Nature *464*, 615–618.
11. Fachinetti, D., Folco, H.D., Nechemia-Arbely, Y., Valente, L.P., Nguyen, K., Wong, A.J., Zhu, Q., Holland, A.J., Desai, A., Jansen, L.E., and Cleveland, D.W. (2013). A two-step mechanism for epigenetic specification of centromere identity and function. Nat. Cell Biol. *15*, 1056–1066.
12. Torras-Llort, M., Medina-Giró, S., Moreno-Moreno, O., and Azorín, F. (2010). A conserved arginine-rich motif within the hypervariable N-domain of Drosophila centromeric histone H3 (CenH3) mediates BubR1 recruitment. PLoS ONE *5*, e13747.
13. Pidoux, A.L., and Allshire, R.C. (2004). Kinetochore and heterochromatin domains of the fission yeast centromere. Chromosome Res. *12*, 521–534.
14. Folco, H.D., Pidoux, A.L., Urano, T., and Allshire, R.C. (2008). Heterochromatin and RNAi are required to establish CENP-A chromatin at centromeres. Science *319*, 94–97.
15. Ishii, K. (2009). Conservation and divergence of centromere specification in yeast. Curr. Opin. Microbiol. *12*, 616–622.
16. Yamagishi, Y., Sakuno, T., Goto, Y., and Watanabe, Y. (2014). Kinetochore composition and its function: lessons from yeasts. FEMS Microbiol. Rev. *38*, 185–200.
17. Bernard, P., Maure, J.F., Partridge, J.F., Genier, S., Javerzat, J.P., and Allshire, R.C. (2001). Requirement of heterochromatin for cohesion at centromeres. Science *294*, 2539–2542.
18. Nonaka, N., Kitajima, T., Yokobayashi, S., Xiao, G., Yamamoto, M., Grewal, S.I., and Watanabe, Y. (2002). Recruitment of cohesin to heterochromatic regions by Swi6/HP1 in fission yeast. Nat. Cell Biol. *4*, 89–93.
19. Steiner, N.C., and Clarke, L. (1994). A novel epigenetic effect can alter centromere function in fission yeast. Cell *79*, 865–874.
20. Pidoux, A.L., Choi, E.S., Abbott, J.K., Liu, X., Kagansky, A., Castillo, A.G., Hamilton, G.L., Richardson, W., Rappsilber, J., He, X., and Allshire, R.C. (2009). Fission yeast Scm3: A CENP-A receptor required for integrity of subkinetochore chromatin. Mol. Cell *33*, 299–311.
21. Cheerambathur, D.K., and Desai, A. (2014). Linked in: formation and regulation of microtubule attachments during chromosome segregation. Curr. Opin. Cell Biol. *26*, 113–122.
22. Tooley, J., and Stukenberg, P.T. (2011). The Ndc80 complex: integrating the kinetochore's many movements. Chromosome Res. *19*, 377–391.
23. Musacchio, A., and Salmon, E.D. (2007). The spindle-assembly checkpoint in space and time. Nat. Rev. Mol. Cell Biol. *8*, 379–393.
24. Hiraoka, Y., Toda, T., and Yanagida, M. (1984). The NDA3 gene of fission yeast encodes beta-tubulin: a cold-sensitive nda3 mutation reversibly blocks spindle formation and chromosome movement in mitosis. Cell *39*, 349–358.
25. Takahashi, K., Chen, E.S., and Yanagida, M. (2000). Requirement of Mis6 centromere connector for localizing a CENP-A-like protein in fission yeast. Science *288*, 2215–2219.
26. Sakuno, T., Tada, K., and Watanabe, Y. (2009). Kinetochore geometry defined by cohesion within the centromere. Nature *458*, 852–858.
27. Ishii, K., Ogiyama, Y., Chikashige, Y., Soejima, S., Masuda, F., Kakuma, T., Hiraoka, Y., and Takahashi, K. (2008). Heterochromatin integrity affects chromosome reorganization after centromere dysfunction. Science *321*, 1088–1091.
28. Carroll, C.W., Milks, K.J., and Straight, A.F. (2010). Dual recognition of CENP-A nucleosomes is required for centromere assembly. J. Cell Biol. *189*, 1143–1155.
29. Kato, H., Jiang, J., Zhou, B.R., Rozendaal, M., Feng, H., Ghirlando, R., Xiao, T.S., Straight, A.F., and Bai, Y. (2013). A conserved mechanism for centromeric nucleosome recognition by centromere protein CENP-C. Science *340*, 1110–1113.
30. Hori, T., Amano, M., Suzuki, A., Backer, C.B., Welburn, J.P., Dong, Y., McEwen, B.F., Shang, W.H., Suzuki, E., Okawa, K., et al. (2008). CCAN makes multiple contacts with centromeric DNA to provide distinct pathways to the outer kinetochore. Cell *135*, 1039–1052.
31. Tanaka, K., Chang, H.L., Kagami, A., and Watanabe, Y. (2009). CENP-C functions as a scaffold for effectors with essential kinetochore functions in mitosis and meiosis. Dev. Cell *17*, 334–343.

32. Malvezzi, F., Litos, G., Schleiffer, A., Heuck, A., Mechtler, K., Clausen, T., and Westermann, S. (2013). A structural basis for kinetochore recruitment of the Ndc80 complex via two distinct centromere receptors. EMBO J. *32*, 409–423.
33. Nishino, T., Rago, F., Hori, T., Tomii, K., Cheeseman, I.M., and Fukagawa, T. (2013). CENP-T provides a structural platform for outer kinetochore assembly. EMBO J. *32*, 424–436.
34. Earnshaw, W.C., Sullivan, K.F., Machlin, P.S., Cooke, C.A., Kaiser, D.A., Pollard, T.D., Rothfield, N.F., and Cleveland, D.W. (1987). Molecular cloning of cDNA for CENP-B, the major human centromere autoantigen. J. Cell Biol. *104*, 817–829.
35. Okada, T., Ohzeki, J., Nakano, M., Yoda, K., Brinkley, W.R., Larionov, V., and Masumoto, H. (2007). CENP-B controls centromere formation depending on the chromatin context. Cell *131*, 1287–1300.
36. Hellwig, D., Munch, S., Orthaus, S., Hoischen, C., Hemmerich, P., and Diekmann, S. (2008). Live-cell imaging reveals sustained centromere binding of CENP-T via CENP-A and CENP-B. J. Biophotonics *1*, 245–254.
37. Hori, T., Shang, W.H., Toyoda, A., Misu, S., Monma, N., Ikeo, K., Molina, O., Vargiu, G., Fujiyama, A., Kimura, H., et al. (2014). Histone H4 Lys 20 monomethylation of the CENP-A nucleosome is essential for kinetochore assembly. Dev. Cell *29*, 740–749.
38. Sanders, S.L., Portoso, M., Mata, J., Bähler, J., Allshire, R.C., and Kouzarides, T. (2004). Methylation of histone H4 lysine 20 controls recruitment of Crb2 to sites of DNA damage. Cell *119*, 603–614.